Research Article

Sumayah H. Alhejaili, Haza S. Alayachi, Fisal A. H. Asiri, Abdulghani R. Alharbi, and Aly R. Seadawy*

Analytical and numerical investigation of exact wave patterns and chaotic dynamics in the extended improved Boussinesq equation

https://doi.org/10.1515/phys-2025-0146
received January 09, 2025; accepted March 11, 2025

Abstract: The study employs sophisticated numerical and analytical methods to examine contemporary approaches to the improved Boussinesq equation. Initially, we concentrate on the exact solutions derived from modifying the Kudryashov and improved generalized Riccati equation mapping approaches, which delineate diverse soliton solutions that facilitate further generalization. These methods make it possible to deepen the understanding of the equation of physical nature as well as provide a dependable means of conducting parametric studies of nonlinear systems. We also created a mesh as the solving tool to the equation to test how the equation would respond under different operating conditions. Numerical solutions are demonstrated with analytical solutions that are generated using Taylor expansion methods whereby, analytical solutions follow the Von Neumann method for stability analysis so as to minimize the capability and confirm the two approaches of solutions. It has been shown in this work that the two methods of solving nonlinear equation gave appropriate results and are suitable for other nonlinear evolutionary systems.

Keywords: improved Boussinesq equation, soliton solutions, dynamic behaviors in nonlinear systems, numerical solution, adaptive moving mesh, nonlinear evolutionary systems

*** Corresponding author: Aly R. Seadawy,** Mathematics Department, Faculty of Science, Taibah University, Al-Madinah Al-Munawarah, 41411, Saudi Arabia, e-mail: aabdelalim@taibahu.edu.sa
Sumayah H. Alhejaili: Mathematics Department, Faculty of Science, Taibah University, Al-Madinah Al-Munawarah, 41411, Saudi Arabia, e-mail: sumayah.hamzah11@gmail.com
Haza S. Alayachi: Mathematics Department, Faculty of Science, Taibah University, Al-Madinah Al-Munawarah, 41411, Saudi Arabia, e-mail: hsshareef@taibahu.edu.sa
Fisal A. H. Asiri: Mathematics Department, Faculty of Science, Taibah University, Al-Madinah Al-Munawarah, 41411, Saudi Arabia, e-mail: fahasiri@taibahu.edu.sa
Abdulghani R. Alharbi: Mathematics Department, Faculty of Science, Taibah University, Al-Madinah Al-Munawarah, 41411, Saudi Arabia, e-mail: arharbi@taibahu.edu.sa

1 Introduction

Joseph Boussinesq presented the Boussinesq equation in 1873 [1], which is expressed as follows:

$$\Theta_{tt} - \Theta_{xx} - \Theta_{xxxx} - (\Theta^2)_{xx} = 0. \tag{1}$$

Such equation is typical to a range of nonlinear dispersive wave phenomena, including propagation of long waves in shallow water, one-dimensional nonlinear lattices, and ion-sound waves in uniform isotropic plasma [2]. This result has basic applicability in actual physics. The words x and t are understood as spatial and temporal coordinates, respectively, and c is a real constant, which in the literature when $c = -1$ is commonly known as the good Boussinesq equation or the well-posed equation [4] in this context.

On the other hand, when it is equal to one, that type of equation is recognized as the bad Boussinesq equation or the ill-posed classical equation [1,5]. Such modified version published by Bogolubsky [6] makes it possible to replace the term Θ_{xxxx} with Θ_{xxtt}. This results in the improved Boussinesq equation and takes the following form:

$$\Theta_{tt} - \Theta_{xx} - c\Theta_{xxtt} - (\Theta^2)_{xx} = 0. \tag{2}$$

The improved Boussinesq equation allows for improvements over the original model, which provides the more realistic interaction of different physical processes such as the wave propagation perpendicular to magnetic field lines [5], ion-sound waves [7], and acoustic waves in elastic rods [8]. Furthermore, this equation is also stably numerical, which increases its fitness for implementation in computer simulations so that the description of its solutions becomes more holistic [6].

This article particularly focuses on the enhanced Boussinesq equation, which this time has been taken from multiple authors like previous studies [15–18]. The improved Boussinesq equation is expressed as follows:

$$\Theta_{tt} - \Theta_{xxtt} - \Theta_{xx} - \Theta\Theta_{xx} - (\Theta_x)^2 = 0. \tag{3}$$

We can express Eq. (4) in the following form:

$$\Theta_{tt} - \Theta_{xxtt} - \Theta_{xx} - \frac{1}{2}(\Theta^2)_{xx} = 0. \tag{4}$$

This is a nonlinear partial differential equation (PDE), more precisely, a kind of the enhanced Boussinesq equation that governs wave propagation in nonlinear dispersive media systems. Θ_{tt} (second derivative of Θ with respect to time) refers to the wave acceleration, which explains how the wave velocity changes within the period of time. In fact, this is a common term found in wave equations as it is concerned with the temporal nature of the wave. Θ_{xxtt} (second derivative of the Θ function in time and space) concerns with the effects of change over time and over space. In this case, it describes the time effect of the wave, more particularly the space effect on the time effect of the wave's curvature. This is an often encountered term in modified wave equations such as the enhanced Boussinesq equation, where dispersion is dominant in wave characteristics. Θ_{xx} (second spatial derivative of Θ) is captured the spatial curvature of the wave, reflecting its local deformation in space. Physically, it describes how the wave spreads out or bends during propagation. In wave dynamics, such terms often represent restoring forces (such as tension or pressure) that work to smooth out the wave's profile. The expression $-\frac{1}{2}(\Theta^2)_{xx}$, which includes the nonlinear term $(\Theta^2)_{xx}$, demonstrates the dependency of wave propagation on the amplitude of a wave. The squaring of this term brings about nonlinearity in a way that the greater the amplitude, the more impact certain behaviors of the wave would possess. This is a property that occurs in some nonlinear wave equations, and it is linked to wave-sharpness and the formation of solitons, stationary waves that are self-reinforcing localized distinct patterns. This equation describes the behavior of nonlinear dispersive waves and incorporates, apart from the nonlinear term $(\Theta^2)_{xx}$, also dispersion effects, which are caused by the Θ_{xxtt} term. Generally, as waves propagate, the nonlinear effect makes waves grow steeper, while the dispersive effect makes them widen. Such dual cooperation of effects may result in producing solitary waves or solitons, self-reinforced localized waves that propagate over long distances without changing their shape. These kinds of equations are widely used in several disciplines such as fluid mechanics (for the case of shallow water wave descriptions), plasma physics (*e.g.*, ion sound waves), and lattice dynamics (where nonlinear force interactions occur between particles) [10–12]. The present study aims at examining exact wave patterns and investigating the corresponding exact solutions to the extended improved Boussinesq equation. Specifically, the key objective is to understand how solutions representing stationary or traveling waves in definite conditions can be obtained using numerical and analytical approaches [13,14]. The G'/G expansion method and semi-classical approximation methods have also been used by previous authors to extract these solutions [15–18]. But now some new developments in numerical algorithms, say, modified Kudryashov method or enhanced Riccati equation mapping, allow better quality of determination of wave patterns owing to a more generalized outlook of physical processes. Twists and turns are constant studying of this research as they involve the study of chaotic dynamics, which is quite a common phenomenon in physics. Waves interacting within a complex system will always give rise to chaotic systems due to the fact that they are nonlinear in structure. Such chaos should actually be anticipated in any system, which is governed by an nonlinear partial differential equations such as the improved Boussinesq equation. Based on the mathematical analysis and numerical simulation, this work intends to show the regions of chaotic solutions and in addition show the distribution of wave solutions in the presence of nonlinear interactions between them. It is possible to greatly change the solutions of chaos model just by changing the initial conditions slightly. Therefore, accomplishing such tasks immediately necessitates the need of accurate techniques to capture and monitor chaotic solutions and their stability.

So far, many different numerical approaches have been considered for solving the improved Boussinesq equation. These include the finite difference method [2,3], the finite element method [19], finite volume element method [20], and spectral methods [21]. In this work, we improve those approaches, for example, using adaptive moving meshes and uniform meshes that increase the accuracy of the solution and reduce the degree of numerical errors in cases when the solution is chaotic. The recent achievements available in the literature have also provided significant impetus for this investigation. The major aim of this study is to find these traveling wave solutions of the enhanced Boussinesq equation with the use of the modified Kudryashov method and improved generalized Riccati equation mapping (IGREM) method [22–25]. These methods produce an impressive array of traveling wave solutions in the form of trigonometric functions for the wave equations, which will enable the better explanation of complicated phenomena and the dynamics behind them [26–29]. In addition, this article applies adaptive moving mesh and uniform mesh techniques to Eq. (4) to obtain numerical solutions. It is important to note that the initial conditions for the numerical scheme are derived from the

exact solutions. The key idea of the numerical approach is to allocate mesh points in regions of high curvature in the solution to enhance accuracy. While many researchers have focused on obtaining analytical solutions for the improved Boussinesq equation, few have concentrated on achieving accurate numerical solutions to minimize errors. The adaptive moving mesh method [31] effectively distributes mesh points more densely in areas with high error, thereby reducing numerical inaccuracies. This method, frequently employed in numerical algorithms, enhances the accuracy of the outcomes significantly. Accuracy is one of the most important elements in conducting any scientific work, and in this study, exact and numerical solutions are analyzed to provide correctness and reliability. In contrast with many other investigations that focus only on the exact solutions, this study adopts a more prudent approach by supporting the numerical solutions with the exact ones.

The layout of this article is as follows. In Section 2, an analytical solution of Eq. (4) is presented. In Section 3, the approximative treatment of the combined problem (24) is described, with particular attention given to fixed mesh and adaptive moving mesh approaches. Also, such section presents the complete interpretation of the results obtained as well as the discussion. Finally, Section 4 recalls the most important results and conclusions of this work.

2 Reduction and solution of the improved Boussinesq equation using nonlinear methods

This section discusses exact solutions of the improved Boussinesq equation using the modified Kudryashov method and the IGREM approach. These methods are employed to find soliton solutions to nonlinear evolution equations:

$$\psi_1(\Theta, \Theta_t, \Theta_{xx}, \Theta_{xxt}, \Theta_{xxx}, \ldots) = 0, \tag{5}$$

where $\Theta = \Theta(x, t)$ is an unknown function of space x and time t. Various partial derivatives such as Θ_{xx}, Θ_{xxt}, and Θ_{xxx} are involved in Eq. (5). The wave transformation

$$\Theta(x, t) = \hat{\Theta}(\zeta), \quad \zeta = x - st, \tag{6}$$

is applied to reduce the complexity of the PDE. The transformation introduces a new function $\hat{\Theta}(\zeta)$, where ζ is a traveling wave coordinate, where s is the wave speed. This reduces the PDE into an ordinary differential equation (ODE) expressed as

$$\psi_2(\hat{\Theta}, \hat{\Theta}_\zeta, \hat{\Theta}_{\zeta\zeta}, \hat{\Theta}_{\zeta\zeta\zeta}, \hat{\Theta}_{\zeta\zeta\zeta\zeta}, \ldots) = 0. \tag{7}$$

Substituting the wave transformation into the original equation leads to the following ODE:

$$s^2\hat{\Theta}_{\zeta\zeta} - s^2\hat{\Theta}_{\zeta\zeta\zeta\zeta} - \hat{\Theta}_{\zeta\zeta} - \frac{1}{2}(\hat{\Theta}^2)_{\zeta\zeta} = 0, \tag{8}$$

which includes various terms such as $s^2\hat{\Theta}_{\zeta\zeta}$ and $\hat{\Theta}_{\zeta\zeta\zeta\zeta}$. To solve this equation, the homogeneous balancing principle is applied, balancing the highest-order derivative term with the nonlinear term. From this, the value $m = 2$ is determined, and two different strategies will be used to solve the equation, which are presented in the subsequent sections.

2.1 Modified Kudryashov method

The modified Kudryashov method is an enhanced technique used to solve nonlinear evolution equations, building upon the traditional Kudryashov method [33]. The central improvement in the modified version involves replacing the natural exponential base e with an arbitrary base A [32,34]. Such a modification enhances the ability of problem solvers to deal with some nonlinear equations as more flexibility is provided by the freedom to choose an arbitrary base to suit the structure of the equation. Within this framework, a solution of a nonlinear evolution equation, for example, of Eq. (7), is constructed as a polynomial of the form:

$$\hat{\Theta}(\zeta) = \sum_{i=0}^{m} r_i \Upsilon(\zeta)^i, \tag{9}$$

where r_i are the constant values, $\Upsilon(\zeta)$ is a necessary function that remains to be solved for, and m is the polynomial degree of the polynomial. The function $\Upsilon(\zeta)$ satisfies the following differential equation:

$$\Upsilon'(\zeta) = (\Upsilon(\zeta)^2 - \Upsilon(\zeta))\ln(A), \tag{10}$$

where A is a constant that must satisfy two conditions, $A > 0$ and $A \neq 1$. This step provides a generalization of a common function used in the process of nonlinear differential equations, expanding the resolution's reach outside the conventional principles. The solution to this differential Eq. (10) is sought

$$\Upsilon(\zeta) = \frac{1}{1 + \nu A^\zeta}, \tag{11}$$

where ν is an arbitrary constant. This form allows the nonlinear evolution equation to take a more manageable algebraic form. Using the modified Kudryashov method with $m = 2$, the solution can be written as follows:

$$\hat{\Theta}(\zeta) = r_0 + r_1 Y(\zeta) + r_2 Y(\zeta)^2. \tag{12}$$

When inserting this solution into the initial equation and using the characteristics of $Y(\zeta)$, the problem is reduced to a problem of a system of algebraic equations in terms of r_0, r_1, and r_2. The solutions of these equations are the exact solutions of the nonlinear problem, thus confirming the efficiency of the modified Kudryashov method.

This technique from a physicist perspective is also offering much flexibility that can be of much importance in systems where the behavior or the dynamics do not conform to traditional exponential perspective. When modeling physical systems, it is often seen that wave propagation and reaction–diffusion processes contain scaling laws, which make arbitrary base A more intuitive. This extra parameter can be useful to incorporate elaborate solutions in modeling nonlinear complex phenomena, and hence, the technique is of great use in several applications. For a certain class of nonlinear systems, characterized by reacting amplitude-dependent logarithmic terms, we derive precise traveling wave solutions.

1) The analysis begins with the assumption $a_0 = 0$ thus putting aside possible constant contributions to the system dynamics and focusing attention on the nonlinear behavior responsible by the values a_1 and a_2. The constants a_1 and a_2 are expressed as follows:

$$a_1 = \frac{-12\ln^2(A)}{\ln^2(A) - 1}, \quad a_2 = \frac{12\ln^2(A)}{\ln^2(A) - 1},$$

which capture the effect of the amplitude A on the system's oscillatory modes. These parameters demonstrate a nonlinear dependence on A, indicating the system's logarithmic responsiveness to changes in amplitude. The traveling wave s speed is determined by the following relationship:

$$s = \frac{-1}{\sqrt{1 - \ln^2(A)}},$$

showing that the amplitude and wave speed have a nontrivial dependency relation. The limiting speed of the wave increases without bound as $\ln^2(A)$ approaches 1; this is typically understood as a point of a critical parameter in the system where change in wave behavior is likely to occur. Such a critical behavior points toward the possibility of phase transitions or bifurcations in the response of the system. The corresponding exact traveling wave solution is given by

$$\Theta_1(x, t) = -\frac{12v\ln^2(A)A^{st+x}}{(\ln^2(A) - 1)(vA^{st+x} + 1)^2}. \tag{13}$$

The solution achieved here features strongly nonlinear traveling waves, whereby the amplitude and factors associated with its propagation are logarithmic functions of A. From the form of the solution, however, it can be expected that such waves may be either amplified or damped depending on the coupling of the nonlinear terms. In particular, the squared denominator implies that some parts of the space-time could be dominated by strong damping of the oscillations, while other parts like the poles could promote further the oscillations, provided that the conditions at the poles are right.

This derived solution has its importance in explaining wave propagation phenomena within the nonlinear system and especially the critical or singular behavior of that system as the amplitudes approach predetermined thresholds. Such solutions have applications in various branches of physics such as hydrodynamics, plasmoids, nonlinear optics, among many others, where the relationship between amplitude speed and the nonlinearity is indeed a key factor in determining the responses of the system to various measures. It accommodates a stable and iterative wave form over certain bounded ranges where it is dominant the behavior of the system is related to certain parameters. For example, where $\ln^2(A)$ is less than the critical value of 1, it implies that the interpreted wave speed is very well defined; hence, the wave propagates in a consistent or rather orderly manner. This is a specific kind of waveform, in which the patterns are consistent and motion is stable. As the value of $\ln^2(A)$ approaches 1, the wave is associated with chaotic dynamics. This is the point where the critical wave speed becomes undefined, thus pointing to transition points of the wave in the system. From the viewpoint of "chaotic dynamics," it may be viewed as a point that marks a transitory phase between order and chaos. Chaos appears when the wave starts becoming oscillatory with no fixed manner – in which the wave may or may not subsequently get "turned" or pass through the peak or nadir in reference to the time and the space relationship to the amplitude.

2) For the case where $a_0 = \frac{-2\ln^2(A)}{\ln^2(A)+1}$, $a_1 = 0$, and $a_2 = 0$, the traveling wave equation simplifies significantly. The wave speed s is

$$s = \frac{-1}{\sqrt{\ln^2(A) + 1}},$$

signifying that there is a nonlinear relationship between the wave speed and the amplitude A would repeat the sign. Given the aforementioned characteristics, the form provides an accurate and easy description for the motion of the wave within a nonlinear medium.

The corresponding solution for the traveling wave is

$$\Theta_2(x,t) = -\frac{2\ln^2(A)}{\ln^2(A)+1}. \tag{14}$$

This solution describes a wave and explains that its amplitude is a logarithmic function of A, which does not change with time or space. Since the solution does not vary with either x or t, it indicates that the wave configuration is uniform (stationary) and resolution of space and time variables is not required. Here, a stable wave configuration is emphasized and is determined only by amplitude A. It depicts a stable wave where the wave is solely a function of time or space. This precise wave pattern represents a stationary wave, which behaves consistently. Despite the stability presented in the solution, chaotic dynamics might develop when the amplitude A is at a critical value or when small disturbances occur. Chaotic dynamics of nonlinear systems are often state dependent.

3) For the case where

$$a_0 = \frac{-2\ln^2(A)}{\ln^2(A)+1}, \quad a_1 = \frac{12\ln^2(A)}{\ln^2(A)+1},$$
$$a_2 = \frac{-12\ln^2(A)}{\ln^2(A)+1}, \quad \text{and} \quad s = \frac{-1}{\sqrt{\ln^2(A)+1}}.$$

The corresponding solution for the traveling wave is

$$\Theta_3(x,t) = -\frac{2\ln^2(A)(v^2A^{2(-st+x)} - 4vA^{-st+x} + 1)}{(\ln^2(A)+1)(vA^{-st+x}+1)^2}. \tag{15}$$

This solution captures the intricacy of wave interactions between A, which includes the amplitude, space x, and time t. The characteristic of the wave and its velocity of propagation is affected by even small variations in the amplitude A, which also exposes the degree of sensitivity of the system to any change in A. Under specific conditions, these dynamics can produce stable and predictable wave patterns known as "exact wave patterns." However, any small variations in the initial conditions or amplitude A can lead to chaotic behavior, where the wave's motion becomes irregular and unpredictable.

4) In the case where $a_0 = \frac{-2\ln^2(A)}{\ln^2(A)+1}$, $a_1 = \frac{12\ln^2(A)}{\ln^2(A)+1}$, and $a_2 = \frac{-12\ln^2(A)}{\ln^2(A)+1}$, the exact solution for the traveling wave is derived as follows. The wave speed is given by

$$s = \frac{1}{\sqrt{\ln^2(A)+1}},$$

which demonstrates the nonlinear dependence of the wave speed on the amplitude A.
The corresponding solution for the traveling wave is

$$\Theta_4(x,t) = -\frac{2\ln^2(A)(v^2A^{2x} - 4vA^{st+x} + A^{2st})}{(\ln^2(A)+1)(A^{st}+vA^x)^2}. \tag{16}$$

This solution describes complex wave dynamics with nonlinear interactions between the amplitude A, spatial position x, and time t. The exponential terms and the multiple factors involving A highlight that the wave's shape and propagation are highly sensitive to changes in A, x, and t, leading to intricate wave behavior depending on the specific values of these parameters.

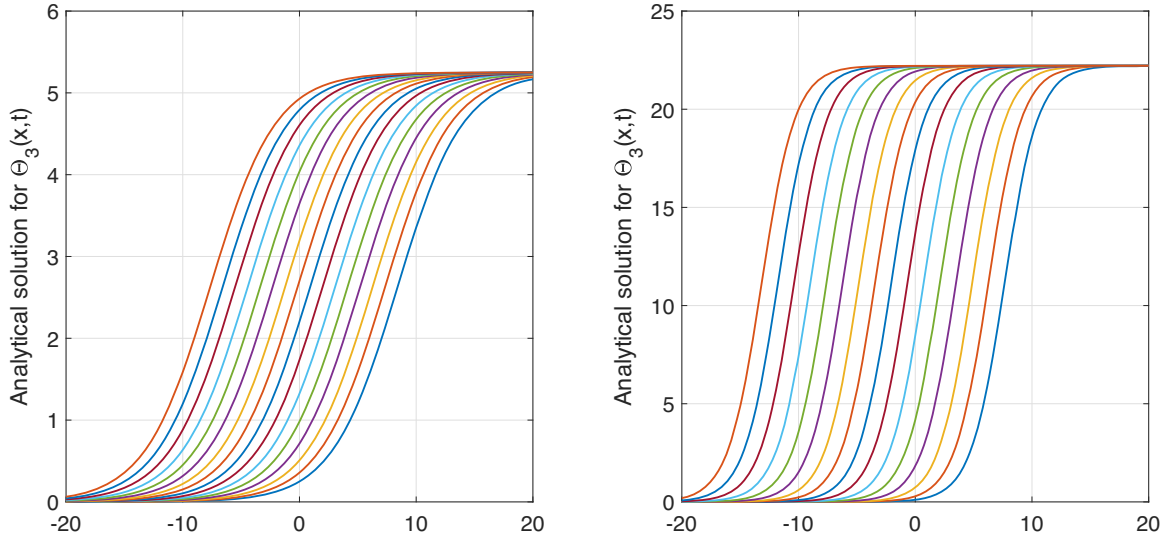

Figure 1: Modified Kudryashov method was used to obtain 2D plots of the analytical solutions to Eq. (4): (left) The parameters are given by $A = 0.7$, $v = 20$, $x_0 = -4$ with $t = 0 \to 15$, $N = 1{,}000$, and $x = -20 \to 20$, and (right) the right plot shows the behavior when $A = 0.5$, $v = 200$.

Figure 1 represents the analytical solutions to a certain equation, obtained using the modified Kudryashov method. These 2D plots offer insights into the behavior of the studied system with varying time and spatial variables. Each colored curve in both plots represents the evolution of an analytical wave solution over time and space. The horizontal axis represents the position x, while the vertical axis represents the analytical solution of the wave $\Theta_3(x, t)$ at specific time values t. In Figure 1 (left), the parameters are given as $A = 0.7$, $v = 20$, and $x_0 = -4$, with time ranging from $t = 0$ to $t = 15$, the number of points $N = 1{,}000$, and space ranging from $x = -20$ to $x = 20$. Physically, this figure reflects an exact wave pattern, where the wave's movement through space and time is regular and stable. All the curves show that the system exhibits predictable behavior, where the wave gradually rises and reaches a steady value. This indicates a stable, predictable wave behavior known as exact wave patterns in nonlinear systems. In Figure 1 (right), the parameters are changed to $A = 0.5$ and $v = 200$. It can be noted that the right curves have a larger dispersion and a greater degree of variability than the left one, which is indicative the higher velocity v causes more irregular and intricate oscillations. This may be indicative of the beginning of chaos. The increase of the velocity v leads to greater nonlinear coupling of the amplitude and spatial modulation, which manifests in chaotic dynamics in which the waves undergo irregular oscillations of varying periods.

2.2 IGREM method

In this section, we present the IGREM approach, which is quite effective in solving nonlinear differential equations [36–38]. The motivation for this approach is to develop a consistent and practical technique that is useful in addressing complex equations, which are common in many applied mathematics areas. We shall investigate the structure as well as the usage of the IGREM technique in details. The IGREM method is used on the equation to rewrite Eq. (7) as

$$\hat{\Theta}(\zeta) = v_0 + \sum_{i=1}^{m} v_i \Phi^i(\zeta), \quad v_i \neq 0, \ i = 1, 2, 3, \ldots, m,$$

where v_i are the arbitrary constants. The function $\Phi(\zeta)$ satisfies the following nonlinear differential equation:

$$\Phi'(\zeta) = \sigma\Phi(\zeta)^2 + \gamma\Phi(\zeta) + \rho. \tag{17}$$

From a general perspective, it is a scaled Riccati equation. In the case when $\rho = 0$ and $\gamma = 0$, Eq. (17) is in the simplest form of a Riccati or Bernoulli equation, which is a standard equation in many mathematical models.

2.2.1 Solutions to the Riccati equation

The solutions to Eq. (17) depend on the discriminant $\mu = \gamma^2 - 4\rho\sigma$. Two cases arise:

Case 1: If $\mu = \gamma^2 - 4\rho\sigma > 0$ with $\rho \neq 0$ or $\gamma\sigma \neq 0$, the solution is given by

$$\Phi(\zeta) = \sqrt{\mu}\tanh\left(\frac{\sqrt{\mu}(\zeta + \zeta_0)}{2}\right) - \frac{\gamma}{2\sigma},$$

or alternatively,

$$\Phi(\zeta) = -\sqrt{\mu}\tanh\left(\frac{\sqrt{\mu}(\zeta + \zeta_0)}{2}\right) \pm i\ \mathrm{sech}\left(\frac{\sqrt{\mu}(\zeta + \zeta_0)}{2}\right) - \frac{\gamma}{2\sigma}.$$

Case 2: If $\mu = \gamma^2 - 4\rho\sigma < 0$ with $\rho \neq 0$ or $\gamma\sigma \neq 0$, the solution takes the form:

$$\Phi(\zeta) = \sqrt{-\mu}\tan\left(\frac{\sqrt{-\mu}(\zeta + \zeta_0)}{2}\right) - \frac{\gamma}{2\sigma},$$

or alternatively,

$$\Phi(\zeta) = -\sqrt{-\mu}\cot\left(\frac{\sqrt{-\mu}(\zeta + \zeta_0)}{2}\right) - \frac{\gamma}{2\sigma}.$$

2.2.2 Traveling wave solutions

Taking into account that the homogeneous balance is $m = 2$, the final form of the traveling wave solution can be expressed as

$$\hat{\Theta}(\zeta) = v_0 + v_1\Phi(\zeta) + v_2\Phi(\zeta)^2. \tag{18}$$

Substituting Eq. (18) into Eq. (4) and simplifying, we derive a system of algebraic equations. Solving this system yields the corresponding soliton solutions. The exact traveling wave solutions are obtained for different families, depending on the discriminant $\mu = \gamma^2 - 4\rho\sigma$ and associated conditions:

Family 1: When $\mu = \gamma^2 - 4\rho\sigma > 0$ and $\rho \neq 0$, the solutions are divided into two cases:

Case 1:

$$\Theta_5(x, t) = -\frac{3\mu\,\mathrm{sech}^2\left(\frac{1}{2}\sqrt{\mu}(x_0 - st + x)\right)}{\mu - 1}, \tag{19}$$

Case 2:

$$\Theta_6(x,t) = \frac{6i\mu}{(\mu-1)(\sinh(\sqrt{\mu}(x_0 - st + x)) - i)}. \quad (20)$$

Family 2: When $\mu = \gamma^2 - 4\rho\sigma < 0$, $\rho\sigma \neq 0$, the solutions are divided into two cases:

Case 3:

$$\Theta_7(x,t) = -\frac{3\mu \sec^2\left(\frac{1}{2}\sqrt{-\mu}(x_0 - st + x)\right)}{\mu - 1}. \quad (21)$$

Case 4:

$$\Theta_8(x,t) = -\frac{3\mu\csc^2\left(\frac{1}{2}\sqrt{-\mu}(x_0 - st + x)\right)}{\mu - 1}. \quad (22)$$

The IGREM method provides an effective framework for deriving exact traveling wave solutions to nonlinear differential equations. By examining different cases based on the discriminant μ, we obtain explicit analytical solutions that can be applied to various physical models exhibiting soliton behavior.

Figures 3(a) and 4(a) display the 3D and 2D plots for Θ_5, respectively, demonstrating how the solutions evolve over the time interval from 0 to 20.

Figure 2 depicts the analytical solution $\Theta_5(x,t)$ obtained using the IGREM method, showcasing exact wave patterns characteristic of solitary waves (solitons) in nonlinear systems. In the 3D plot, the wave moves along the x-axis, preserving its localized structure over time, indicating energy conservation and stability. The 2D plot displays the wave profile at different time steps, further emphasizing the wave's stability and lack of deformation. These solutions highlight the precise nature of solitons, where the interplay between nonlinearity and dispersion allows the wave to maintain its shape during propagation. However, in nonlinear systems, chaotic dynamics can emerge under specific conditions, such as perturbations or variations in system parameters, leading to irregular and unpredictable wave behavior. This transition from exact solutions to a simultaneous understanding of many phenomena is vital to the theory of nonlinear waves in a shallow water area.

3 Numerical results

In tthis section, we utilize two numerical techniques, namely, the uniform mesh method and the adaptive moving mesh method, to compute the numerical solutions for Eq. (4). To facilitate this, we define the function Ω as follows:

$$\Omega = \Theta_t - \Theta_{xxt}, \quad (23)$$

where Θ_t is the time derivative of the numerical solution, and Θ_{xxt} is the mixed domain second-order of the function

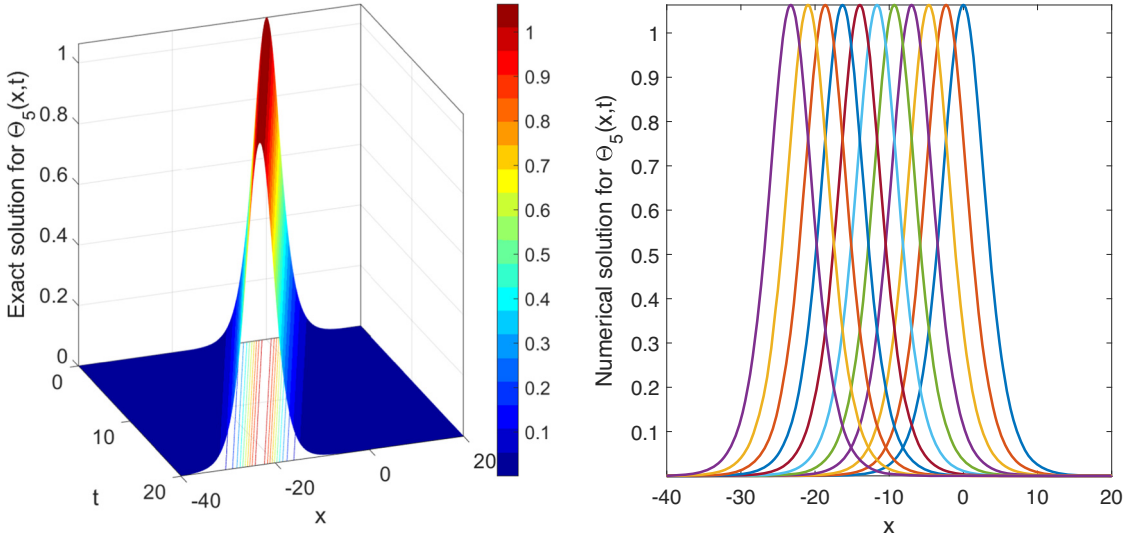

Figure 2: IGREM method was used to find the analytical solution for $\Theta_5(x,t)$. The study parameters were as follows: $\rho = 2.5$, $\sigma = 1.3$, $\gamma = 3.6417$, $x_0 = -8$ with $t = 0 \to 20$, $m_x = 8{,}000$ and $x = -40 \to 20$.

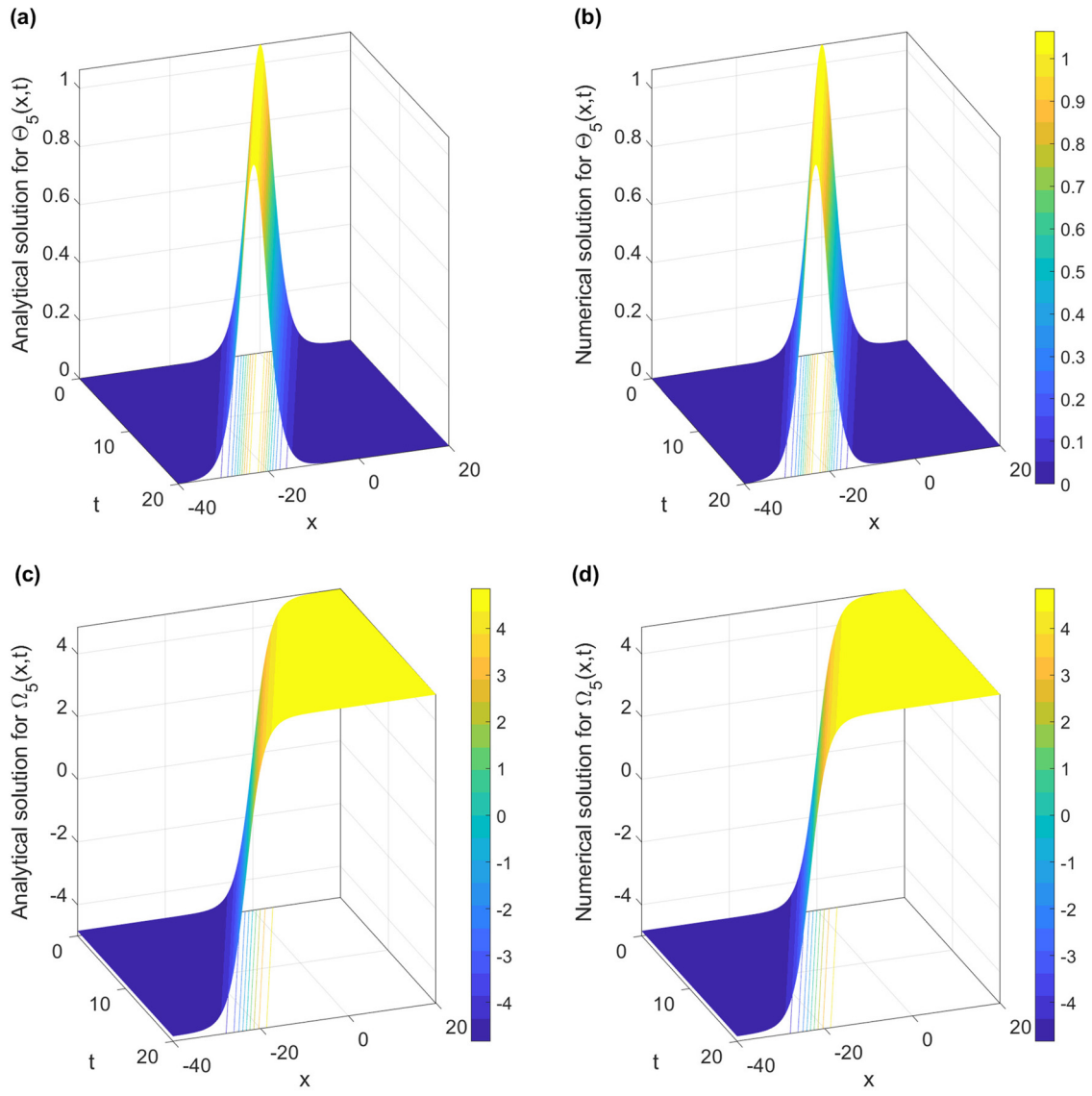

Figure 3: IGREM method was used to find the analytical solution for $\Theta_5(x, t)$ and $\Omega_5(x, t)$, as shown in (a) and (c) as 3D surface plots. (b) and (d) Adaptive moving mesh numerical solution results. The study parameters were as follows: $\rho = 2.5$, $\sigma = 1.3$, $\gamma = 3.6417$, $x_0 = -8$ with $t = 0 \to 20$, $m_x = 8{,}000$, and $x = -40 \to 20$.

of Θ with respect to x and the first-order derivative with respect to the time t. We perform time differentiation on Eq. (23) and substitute this into Eq. (4), thereby obtaining the following system of equations:

$$\begin{aligned} &\Theta_t - \Theta_{xxt} - \Omega = 0, \\ &\Omega_t - \Theta_{xx} - \frac{1}{2}(\Theta^2)_{xx} = 0. \end{aligned} \tag{24}$$

This system serves as the basis for solving the problem numerically. In order to find the numerical solutions, initial conditions are required. Specifically, we determine the initial conditions for Θ by evaluating Eq. (19) at $t = 0$. Once these conditions for Θ are established, we compute the exact solution for $\Omega(x, t)$, given by

$$\Omega(x, t) = \frac{6\sqrt{\mu}\tanh\left[\frac{1}{2}\sqrt{\mu}(x_0 - st + x)\right]}{(-\mu + 1)^{3/2}}. \tag{25}$$

The initial conditions for the system are as follows:

$$\begin{aligned} \Theta(x, 0) &= -\frac{3\mu}{\mu - 1}\operatorname{sech}^2\left[\frac{1}{2}\sqrt{\mu}(x_0 + x)\right], \\ \Omega(x, 0) &= \frac{6\sqrt{\mu}}{(-\mu + 1)^{3/2}}\tanh\left[\frac{1}{2}\sqrt{\mu}(x_0 + x)\right]. \end{aligned} \tag{26}$$

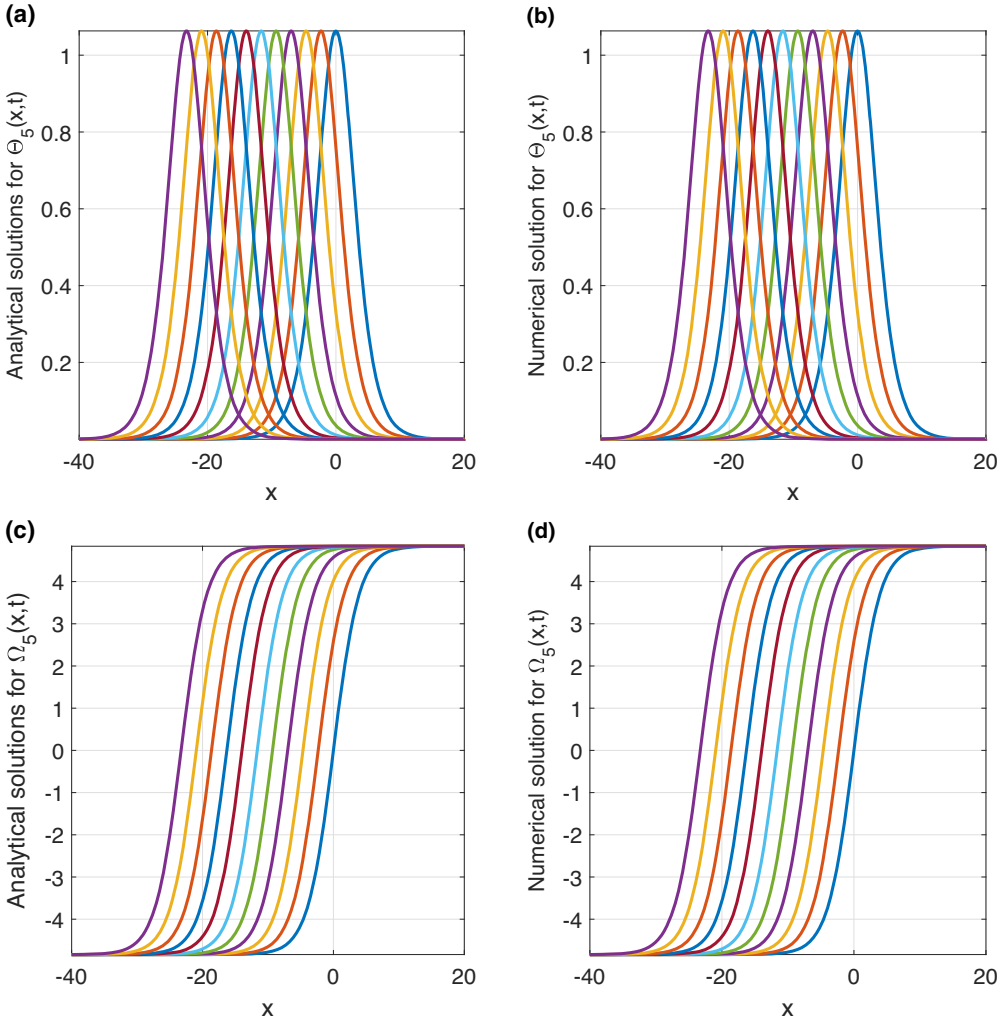

Figure 4: IGREM method was used to find the analytical solution for $\Theta_5(x,t)$ and $\Omega_5(x,t)$, as shown in (a) and (c) as 2D plots. (b) and (d) Adaptive moving mesh numerical solution results. The study parameters were as follows: $\rho = 2.5$, $\sigma = 1.3$, $\gamma = 3.6417$, $x_0 = -8$ with $t = 0 \to 20$, $m_x = 8{,}000$, and $x = -40 \to 20$.

After setting these initial conditions, the uniform mesh or the adaptive moving mesh techniques can be employed to arrive at the numerical solutions while maintaining the analytical solutions.

3.1 Numerical solutions using a uniform mesh

In this section, a uniform mesh method is applied to a physical domain of size $[0, L]$ to obtain numerical solutions for the system in Eq. (24). The domain is divided into m_x subintervals, each of uniform width $\Delta x = \frac{L}{m_x}$, with the points denoted as $[x_i, x_{i+1}]$, where $x_i = (i-1)\Delta x$ for all $x_i \in [0, L]$ and $i = 1, 2, 3, \ldots, m_x + 1$. The discretization of system (24) uses finite difference operators with a uniform subinterval width Δx, and is expressed as follows:

$$\begin{aligned}
&\frac{\Theta_i^{j+1} - \Theta_i^j}{\Delta t} - \frac{1}{\Delta t}((\Theta_{xx})_i^{j+1} - (\Theta_{xx})_i^j) - \Omega_i^{j+1} = 0,\\
&\frac{\Omega_i^{j+1} - \Omega_i^j}{\Delta t} - (\Theta_{xx})_i^{j+1} - \frac{1}{2}(\Theta_{xx}^2)_i^{j+1} = 0,
\end{aligned} \tag{27}$$

where

$$\Theta_{xx} = \frac{\Theta_{i+1} - 2\Theta_i - \Theta_{i-1}}{\Delta x^2},$$

the associated boundary conditions for system (24) are

$$\begin{aligned}
\Theta_{t,1} &= \Theta_{t,m_x+1} = 0,\\
\Omega_{t,1} &= \Omega_{t,m_x+1} = 0.
\end{aligned}$$

The initial conditions are given by

$$\Theta(x,0) = -\frac{3\mu \operatorname{sech}^2\left(\frac{1}{2}\sqrt{\mu}(x_0+x)\right)}{\mu-1},$$
$$\Omega(x,0) = \frac{6\sqrt{\mu}\tanh\left(\frac{1}{2}\sqrt{\mu}(x_0+x)\right)}{(-\mu+1)^{3/2}}.$$

It is important to note that this numerical system is solved using the FORTRAN ODE solver known as the DASPK solver [35].

3.1.1 Stability

In this section, we employ Von Neumann's stability analysis to evaluate the stability of the numerical scheme. System (24) is expressed as

$$\begin{aligned} \Theta_t - \Theta_{xxt} - \Omega &= 0, \\ \Omega_t - \Theta_{xx} - \frac{1}{2}(\Theta\Theta)_{xx} &= 0. \end{aligned} \tag{28}$$

To linearize system (28), we consider the assumption that $C = \Theta(x_i, t_j)$. This simplifies system (28) to

$$\begin{aligned} \Theta_t - \Theta_{xxt} - \Omega &= 0, \\ \Omega_t - \Theta_{xx} - \frac{C}{2}\Theta_{xx} &= 0. \end{aligned} \tag{29}$$

For simplicity, we set $C = 1$, yielding

$$\begin{aligned} \Theta_t - \Theta_{xxt} - \Omega &= 0, \\ \Omega_t - \Theta_{xx} - \frac{1}{2}\Theta_{xx} &= 0. \end{aligned} \tag{30}$$

We can discretize the aforementioned system as

$$\begin{aligned} \Theta_i^{j+1} - \Theta_i^j &= ((\Theta_{xx})_i^{j+1} - (\Theta_{xx})_i^j) + \Delta t \Omega_i^{j+1}, \\ \Omega_i^{j+1} - \Omega_i^j &= \Delta t(\Theta_{xx})_i^{j+1} + \frac{\Delta t}{2}(\Theta_{xx})_i^{j+1}, \\ &\text{where} \\ \Theta_{xx} &= \frac{\Theta_{i+1} - 2\Theta_i - \Theta_{i-1}}{\Delta x^2}. \end{aligned} \tag{31}$$

Next, using the definition from Von Neumann's analysis for Θ_i^j and Ω_i^j, we assume

$$\begin{aligned} \Theta_i^j &= A^j e^{\iota\xi i\Delta x}, \quad \text{and then} \quad \Theta_i^{j+1} = A\Theta_i^j \quad i = 1, 2, 3, \ldots, m_x, \\ \Omega_i^j &= B^j e^{\iota\xi i\Delta x}, \quad \text{and then} \quad \Omega_i^{j+1} = B\Omega_i^j \quad i = 1, 2, 3, \ldots, m_x, \end{aligned} \tag{32}$$

where A and B are the constants. Substituting into system (32) and simplifying yield:

$$\begin{aligned} A\Theta_i^j - \Theta_i^j &= \frac{1}{\Delta x^2}(A\Theta_i^j(e^{\iota\xi\Delta x} - 2 + e^{-\iota\xi\Delta x}) \\ &\quad - \Theta_i^j(e^{\iota\xi\Delta x} - 2 + e^{-\iota\xi\Delta x})) + \Delta t B\Omega_i^j, \\ B\Omega_i^j - \Omega_i^j &= \frac{\Delta t}{\Delta x^2}(A\Theta_i^j(e^{\iota\xi\Delta x} - 2 + e^{-\iota\xi\Delta x})) \\ &\quad + \frac{\Delta t}{2\Delta x^2}(A\Theta_i^j(e^{\iota\xi\Delta x} - 2 + e^{-\iota\xi\Delta x})). \end{aligned} \tag{33}$$

After simplifying Eq. (33), we obtain

$$\begin{aligned} \Theta_i^{j+1} - \frac{\delta_1}{\Delta t}\Theta_i^{j+1} - \Delta t\Omega_i^{j+1} &= \Theta_i^j - \frac{\delta_1}{\Delta t}\Theta_i^j, \\ -\delta_1\Theta_i^{j+1} - \frac{\delta_1}{2}\Theta_i^{j+1} + \Omega_i^{j+1} &= \Omega_i^j, \end{aligned}$$

where

$$\delta_1 = \frac{\Delta t}{\Delta x^2}\left(-4\iota \sin\left(\frac{\xi\Delta x}{2}\right)\right).$$

Thus, we arrive at the final equation

$$\left(1 - \frac{\delta_1}{\Delta t}\right)\Theta_i^{j+1} - \Delta t\Omega_i^{j+1} = \left(1 - \frac{\delta_1}{\Delta t}\right)\Theta_i^j, \tag{34}$$

which simplifies to

$$-1.5\delta_1\Theta_i^{j+1} + \Omega_i^{j+1} = \Omega_i^j. \tag{35}$$

By dividing both sides of Eq. (34) by $\left(1 - \frac{\delta_1}{\Delta t}\right)$, we obtain

$$\begin{aligned} \Theta_i^{j+1} - \frac{\Delta t \quad \Omega_i^{j+1}}{(1 - \frac{\delta_1}{\Delta t})} &= \Theta_i^j, \\ -1.5\delta_1\Theta_i^{j+1} + \Omega_i^{j+1} &= \Omega_i^j, \end{aligned} \tag{36}$$

resulting in the simplified system:

$$\begin{pmatrix} 1 & \frac{-\Delta t}{(1 - \frac{\delta_1}{\Delta t})} \\ -1.5\delta_1 & 1 \end{pmatrix}\begin{pmatrix}\Theta\\ \Omega\end{pmatrix}^{j+1} = \begin{pmatrix}\Theta\\ \Omega\end{pmatrix}^j. \tag{37}$$

This system can be expressed as

$$\begin{pmatrix}\Theta\\ \Omega\end{pmatrix}^{j+1} = G\begin{pmatrix}\Theta\\ \Omega\end{pmatrix}^j, \tag{38}$$

where

$$G = \begin{pmatrix} 1 & \frac{-\Delta t}{(1 - \frac{\delta_1}{\Delta t})} \\ -1.5\delta_1 & 1 \end{pmatrix}^{-1}.$$

According to the Von Neumann's stability criterion, the maximum eigenvalues of the matrix G should be $G \le 1$. Through the use of Mathematical software, it has been established that the eigenvalues of G are as follows:

$$\lambda_{1,2} = \left\{\frac{1}{1 - \frac{\sqrt{1.5\,\delta_1\Delta t^2}}{\sqrt{\delta_1\Delta t^2(\Delta t - \delta_1)}}}, \frac{1}{\frac{\sqrt{1.5\,\delta_1\Delta t^2}}{\sqrt{\delta_1\Delta t^2(\Delta t - \delta_1)}} + 1}\right\}.$$

The Von Neumann stability condition holds for contours such that $|\lambda_{1,2}|^2 \le 1$, which confirms that the scheme is unconditionally stable.

A Taylor expansion is used to determine the accuracy of the finite difference implicit scheme. It has been shown that the scheme possesses first-order accuracy in time (with an

error proportional to Δt) and second-order accuracy in space (with an error proportional to Δx^2). This suggests that the temporal error decreases at a slower rate than the spatial error. This balance of the errors guarantees the applicability of the scheme for numerical simulation, provided that the size of the time and space steps is adequate.

3.2 Adaptive mesh numerical solutions

An adaptive method of a mesh is described to be employed in this section to address the numerical problem of mapping from the computational domain [0,1] to the physical domain $[0, L]$. The mapping is written in the form of $x = x(\eta, t)$, where $\eta : [0,1] \to [0, L]$ for $t > 0$. In this formulation, the following coordinates introduced a physical coordinate, x, and a computational coordinate, η. The variables are defined as

$$\Theta = \Theta(x, t), \quad \Lambda = \Lambda(x, t), \quad \Omega = \Omega(x, t),$$

where the association $x = x(\eta, t)$ applies. The adaptive mesh refinement splits the geometrical area from $x_0 = 0$ to $x_m = L$ into $m + 1$ sub-intervals. The mesh x_i will be given by $x_i = x(\eta_i, t)$, where $\eta_i = \frac{i}{m}$ and $i = 0,1,\ldots, m$. Controlled differentiation allowed us to obtain the following:

$$\dot{\Theta} = \Theta_x \dot{x} - (\Theta_{xx})\frac{\dot{\eta}}{\eta},$$

$$\dot{\Omega} = \Omega_x \dot{x} + \frac{1}{2}(\Omega^2)_x,$$

where Θ_{xx} is computed as

$$\Theta_{xx} = \frac{1}{\eta}\left(\frac{\Theta_\eta}{x_\eta}, \frac{\eta_\eta}{x_\eta}\right).$$

Boundary conditions are set as follows:

$$\Theta_{t,1} = \Theta_{t,m+1} = 0, \quad \Omega_1 = \Omega_{m+1} = 0, \quad \forall t \geq 0.$$

Initial conditions are based on

$$\Theta(\eta, 0) = -3\mu \operatorname{sech}^2\left(\frac{1}{2}\sqrt{\mu}(x_0 + x)\right),$$

$$\Omega(\eta, 0) = 6\sqrt{\mu}\tanh\left(\frac{1}{2}\sqrt{\mu}(x_0 + x)\right).$$

The methodology focuses on minimizing errors and maximizing convergence through different sets of monitoring functions with MMPDE6 [39–41] as the preferred method, which is given as

$$\text{MMPDE6}: x_{t,\eta\eta} = -\frac{1}{\tau}(\varpi x_\eta)_\eta,$$

where $0 < \tau < 1$ is a relaxation parameter and $\varpi(\Theta, \Omega, x)$ is a curvature-dependent monitoring function targeting regions with significant solution variations:

$$\text{Curvature-based monitor function}: \quad \varpi(\Theta, \Omega, x) = (1 + g_1 |\Theta_{xx}|^2 + g_2 |\Omega_{xx}|^2)^{\frac{1}{4}}. \tag{39}$$

The user-specified weight parameters g_1 and g_2 allocate additional nodes to areas with high error. The approach includes discretizing the spatial derivative while maintaining a continuous temporal derivative. The coupled equations are solved using FORTRAN software and ODE solvers, employing finite differences within the adaptive mesh framework to achieve accurate solutions.

The IGREM method results, visualized through 3D surface plots, assess the dynamics of the functions $\Theta(x, t)$ and $\Omega(x, t)$ in relation to exact wave patterns and chaotic dynamics. Analytical solutions (Figure 3(a) and (c)) demonstrate precise, theoretical wave patterns indicative of stable and predictable system behaviors, which are crucial for verifying the accuracy of numerical methods. The numerical solutions (Figure 3(b) and (d)), utilizing an adaptive moving mesh, reflect the system's sensitivity to initial conditions, characteristic feature of chaotic dynamics. The variable mesh density is strategically employed to better capture complex behaviors in areas of high gradient. The observable discrepancies between the analytical and numerical solutions suggest the presence of chaotic dynamics, particularly evident in abrupt changes within the numerical plots. This highlights the method's dual capability to capture both the predictable and intricate behaviors of the modeled system, illustrating the complexities involved in simulating theoretical precision and chaotic dynamics within practical computational frameworks.

4 Results and discussion

This study achieved important outcomes using the modified Kudryashov and IGREM methods to obtain multiple exact solutions for Eq. (4). The analytical results obtained were confronted with the results of earlier works on the same subject in order to relate their accuracy. Such a comparison accentuates the originality of the solutions produced by the modified Kudryashov and IGREM methods since the ones from the study by Yang [18] were different. In their study, [18] utilized the trial equation method to derive traveling wave solutions for the improved Boussinesq equation, expressed solely as trigonometric functions, without the inclusion of solution plots. In contrast, our approach, through the modified Kudryashov method, produces a broader spectrum of traveling wave solutions, notably in logarithmic forms. Similarly, the IGREM method

furnishes multiple solutions encompassing both trigonometric and hyperbolic functions.

Further investigations were conducted into the numerical solutions of the improved Boussinesq system (24) employing two numerical methodologies: the uniform mesh and the adaptive moving mesh methods. It is noteworthy that the improved Boussinesq Eq. (4) was transformed into system (24) to streamline the numerical solution process. Our findings reveal that the uniform mesh scheme (27) attains precise accuracy (t, h^2) while maintaining unconditional stability. Using these exact solutions, we established the initial conditions as outlined in Eq. (26) for the improved Boussinesq system.

The adaptive moving mesh method has demonstrated its efficacy in addressing a broad spectrum of PDEs, particularly effective in solving the improved Boussinesq equation. This method offers highly accurate numerical approximations and substantially reduces computational errors. The comparative analysis between the exact and numerical solutions underscores the efficiency of the adaptive moving mesh method. Results are visually represented in Figures 3 and 4.

In Figure 3, 3D surface plots vividly illustrate the analytical solutions for Θ_5 and Ω_5 in panels (a) and (c), while panels (b) and (d) depict the corresponding numerical solutions. The parameters used in this analysis include $\rho = 2.5$, $\sigma = 1.3$, $\gamma = 3.6417$, $x_0 = -8$ with $t = 0 \to 20$, $m = 8{,}000$, and $x = -40 \to 20$. Figure 4 shows 2D plots of the same solutions, where the analytical solutions for Θ_5 and Ω_5 are displayed in (a) and (c), and the numerical solutions in (b) and (d). These figures clearly demonstrate that both sets of solutions align closely and exhibit similar behaviors, resulting in a negligible error due to its minimal magnitude. Figure 5(a) and (b) presents the time evolution of a solitary wave solution analyzed using the adaptive moving mesh technique with the monitor function and MMPDE6 for $\Theta_5(x, t)$ and $\Omega_5(x, t)$, respectively, over a time span from 0 to 10, with $m_x = 500$. Figure 5(c) displays the equidistributing coordinate transformation $x(\eta)$, where the solid blue line marks the initial uniform mesh. The methodologies proposed herein hold potential for application across a diverse range of nonlinear models in contemporary physics. Figure 3 demonstrates the use of adaptive mesh refinement and the time evolution of a numerical solution. In

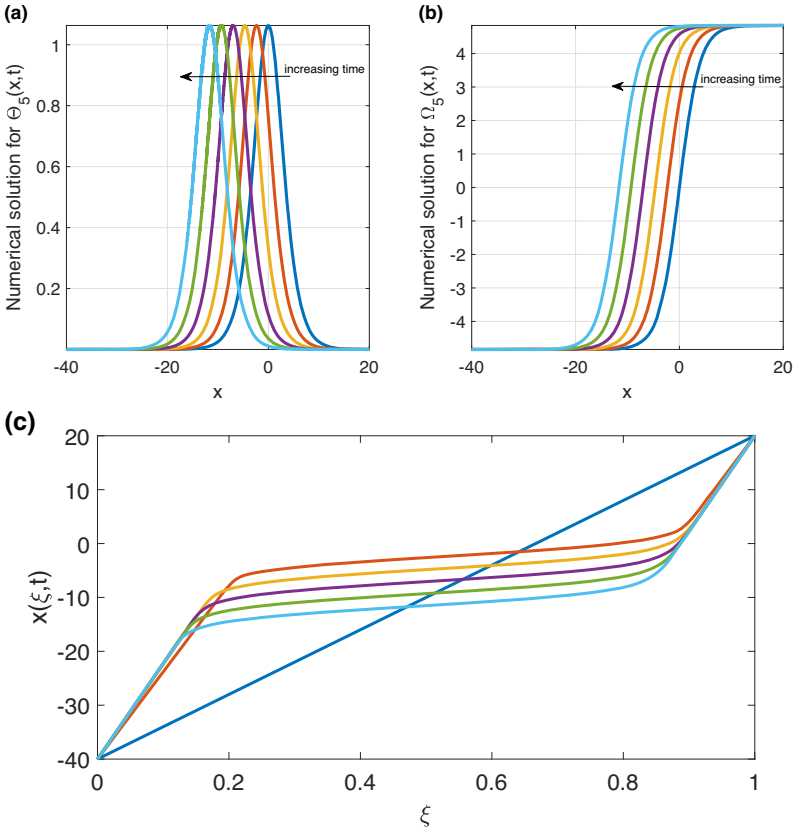

Figure 5: (a) and (b) Time development of a single traveling wave for $\Theta_5(x, t)$ and $\Omega_5(x, t)$. (c) Time evolution of the corresponding mesh x.

Figure 3 (c), mesh points are redistributed, focusing more points in regions where the solution changes rapidly. This method allows for a better approximation in the numerical solutions, notably in the case of interpolating equations of state that present discontinuities, such as those describing the ideal gas or the diffusion of heat in nonhomogeneous solids. To start with, the points are uniformly distributed; however, as time proceeds and the solution becomes more diverse, the overall grid compresses and point concentrations vary with regions of greater gradient for improvement in accuracy. In Figure 3(a) and (b), the change of the numerical solutions with time is shown with space and value of the solution as dependent and independent variables, respectively. Figure 3 gives rise to a belly-shaped curve, which shifts to the y-axis and narrows, which means that some form of diffusion or transmission occurs across space. The curve moves in the left direction with time, which shows the movement of the solution with shape of the curve getting narrower, and therefore, concentration or some form of process, which leads to diffusion of the variable, occurs. This is observed in solutions to problems described, for example, by heat equations or wave equations in the sense that there exists some propagation of heat or sound waves. The spatial correlation between those graphs is also clear: once the solution in the second graph builds up in particular areas, the grid in the first graph, over time, restructures to fit those areas of the solution with rapid change in regions, and hence, accuracy is maintained. The combination of an adaptive mesh refinement with the evolving solutions concept is very important in the solving of differential equations with a very high degree of accuracy.

5 Conclusions

This report presents an exhaustive dimension of the study where the modified Kudryashov method and IGREM methods were exactly used in the search for new traveling wave solutions of the extended improved Boussinesq equation. This study offered exact analytical solutions and also enhanced numerical solutions through adaptive and uniform mesh techniques with a drastic improvement of computational errors in comparison with previous works. The study demonstrated the bifurcation of the systems under investigation indicating both ordered and chaotic characteristics of nonlinear dynamics. Such a result increased our comprehension of the factors governing such systems and particularly, the initial state and the trajectories in the phase space that bears many characteristics of chaotic systems. The adaptive mesh method was very useful in accurately modeling complex wave behaviors in areas of high computation requirement. This method automatically determines the grid points to restrict the amount of errors, which is instrumental in solving differential equations of high complexity. Asserting exact waveforms and chaotic dynamics architectures through the application of IGREM M, the graphical outcomes exhibited both stationary and chaotic dynamics in the systems of interest. This analysis emphasized the efforts of numerical simulations, which are theoretical in nature and evolves toward the complex dynamics of real systems exhibiting both chaos and order. This research pointed to further theoretical developments of the modified equation as well as improved practical tools for nonlinear systems investigation. Our results show that these techniques allow achieving clearcut and efficient solutions, thus broadening the prospects of this research in many domains, for instance, in the dynamics of fluids, material science, geo-processes, or energy problems. As a result, this study is useful in the context of mathematical physics since it progresses the search for apt resources for probing some intricate systems and opens fruitful prospects for further studies, leading eventually to new findings and technology that improves human beings' living condition.

Funding information: The authors state no funding involved.

Author contribution: All authors have accepted responsibility for the entire content of this manuscript and approved its submission.

Conflict of interest: The authors state no conflict of interest.

Data availability statement: The datasets generated and/or analysed during the current study are available from the corresponding author on reasonable request.

References

[1] Boussinesq J. Theorie des ondes et des remous qui se propagent le long daun canal rectangulaire horizontal, en communiquant au liquide contenu dans ce canal des vitesses sensiblement pareilles de la surface au fond. J Math Pures Appl. 1872;17:55–108.

[2] Iskandar L, Jain PC. Numerical solutions of the improved Boussinesq equation. Proc Indian Acad Sci Sect A Phys Sci. 1980;89(3):171–81. doi: 10.1007/bf02861996.

[3] El-Zoheiry H. Numerical study of the improved Boussinesq equation. Chaos Solitons Fract. 2002;14(3):377–84. doi: 10.1016/s0960-0779(00)00271-x.

[4] Manoranjan VS, Mitchell AR, Morris J. Numerical solutions of the good Boussinesq equation. SIAM J Sci Stat Comput. 1984;5(4):946–57. doi: 10.1137/0905065.

[5] Wazwaz A. Partial differential equations and Solitary waves theory. In Nonlinear Physical Science. Springer; 2009. doi: 10.1007/978-3-642-00251-9.
[6] Bogolubsky I. Some examples of inelastic soliton interaction. Comput Phys Commun. 1977;13(3):149–55, doi: 10.1016/0010-4655(77)90009-1.
[7] Christiansen PL, Muto V, Rionero S. Solitary wave solutions to a system of Boussinesq-like equations. Chaos Solitons Fractals. 1992;2(1):45–50. doi: 10.1016/0960-0779(92)90046-p.
[8] Berezin YA, Karpman VI. Nonlinear evolution of disturbances in plasmas and other dispersive media. J Experiment Theoret Phys. 1966;24:1049. https://ui.adsabs.harvard.edu/abs/1967JETP...24.1049B/abstract.
[9] Soerensen MP, Christiansen PL, Lomdahl PS, Skovgaard O. Solitary waves on nonlinear elastic rods. I. J Acoust Soc Am. 1984;76(3):871–9. doi: 10.1121/1.391312.
[10] Öztop HF, Bakir E, Selimefendigil F, Guuur M, Cosssanay H. Effects of İnclined plate in a channel to control melting of PCM in a body -inserted on the bottom wall, S.I. Comput Experim Dynam Complex Fluid Struct. 2023;47:123–37.
[11] Cosssanay H, Oztop HF, Guuur M, Bakir E. Analysis of turbulent wall jet impingement onto a moving heated body. Int J Numer Methods Heat Fluid Flow. 2022;32(9):2938–63. doi: 10.1108/HFF-08-2021-0521.
[12] Gur M, Oztop H, Biswas N, Selimefendigil F. Three-dimensional analysis of turbulent twin-swirling jets onto a heated rectangular prism in a channel. Int J Numer Meth Heat Fluid Flow. 2025;35(3):1137–71. doi: 10.1108/HFF-08-2024-0559.
[13] Seadawy AR, Alsaedi BA. Variational principle and optical soliton solutions for some types of nonlinear Schrödinger dynamical systems. Int J Geomet Methods Modern Phys. 2024;21(6):2430004.
[14] Parasuraman E, Seadawy AR, Muniyappan A. Stability and instability nature of solitons in an optical fiber with four wave mixing effect. Phys Scr. 2024;99:095223.
[15] Yang Z, Hon Y. An improved modified extended tanh-function method. Zeitschrift Für Naturforschung. 2006;61(3–4):103–15. doi: 10.1515/zna-2006-3-401.
[16] Abdou MA, Soliman A, El-Basyony S. New application of Exp-function method for improved Boussinesq equation. Phys Lett. 2007;369(5–6):469–75. doi: 10.1016/j.physleta.2007.05.039.
[17] Abazari R, Kılıçman A. Solitary wave solutions of the Boussinesq equation and its improved form. Math Problem Eng. 2013;2013:1–8. doi: 10.1155/2013/468206.
[18] Yang L. Trial equation method for solving the improved Boussinesq equation. Adv Pure Math. 2014;4(2):47–52. doi: 10.4236/apm.2014.42007.
[19] Lin Q, Wu Y, Loxton R, Lai S. Linear B-spline finite element method for the improved Boussinesq equation. J Comput Appl Math. 2009;224(2):658–67. doi: 10.1016/j.cam.2008.05.049.
[20] Wang Q, Zhang Z, Zhang X, Zhu Q. Energy-preserving finite volume element method for the improved Boussinesq equation. J Comput Phys. 2014;270:58–69. doi: 10.1016/j.jcp.2014.03.053.
[21] Borluk H, Muslu GM. A Fourier pseudospectral method for a generalized improved Boussinesq equation. Numer Methods Partial Differ Equ. 2014;31(4):995–1008. doi: 10.1002/num.21928.
[22] Kumar A, Kumar S, Bohra N, Pillai G, Kapoor R, Rao J. Exploring soliton solutions and interesting wave-form patterns of the (1+1)-dimensional longitudinal wave equation in a magnetic-electro-elastic circular rod. Opt Quant Electron. 2024;56:1029. doi: 10.1007/s11082-024-06901-x.
[23] Kumar A, Kumar S. Dynamical behaviors with various exact solutions to a (2+1)-dimensional asymmetric Nizhnik-Novikov-Veselov equation using two efficient integral approaches. Int J Modern Phys B. 2024;38(5):2450064.
[24] Kumar S, Kumar D, Kumar A. Lie symmetry analysis for obtaining the abundant exact solutions, optimal system and dynamics of solitons for a higher-dimensional Fok's equation. Chaos Solitons Fractals. 2021;142:110507.
[25] Kumar S, Kumar A. Lie symmetry reductions and group invariant solutions of (2 + 1)-dimensional modified Veronese web equation. Nonlinear Dyn. 2019;98:1891–903. doi: 10.1007/s11071-019-05294-x.
[26] Raza A. Ali K Rizvi ATR, Sattar S, Seadawy AR. Discussion on vector control dengue epidemic model for stability analysis and numerical simulations. Brazil J Phys. 2025;55:21.
[27] Arshad M, Seadawy AR, Mehmood A, Shehzad K. Lump Kink interactional and breather-type waves solutions of (3+1)-dimensional shallow water wave dynamical model and its stability with applications. Modern Phys Lett B. 2025;39(1):2450402 (17 pages).
[28] Iqbal M, Lu D, Seadawy AR, Alomari FAH, Umurzakhova Z, Myrzakulov R. Constructing the soliton wave structure to the nonlinear fractional Kairat-X dynamical equation under computational approach. Modern Phys Lett B. 2025;39(2):2450396 (20 pages).
[29] Rizvi STR, Ali K, Akram U, Abbas SO, Bekir A, Seadawy AR. Stability analysis and solitary wave solutions for Yu Toda Sasa Fukuyama equation. Nonlinear Dyn. 2025;113:2611–23.
[30] Almatrafi MB, Alharbi A, Tunç C. Constructions of the soliton solutions to the good Boussinesq equation. Adv Differ Equ. 2020;2020(1):315. doi: 10.1186/s13662-020-03089-8.
[31] Huang W, Russell RD. Adaptive moving mesh methods. Applied Mathematical Sciences. IOP Publishing; 2011. doi: 10.1007/978-1-4419-7916-2.
[32] Srivástava HM, Băeanu D, Machado JAT, Osman MS, Rezazadeh H, Arshed S, et al. Traveling wave solutions to nonlinear directional couplers by modified Kudryashov method. Phys Scr. 2020;95(7):075217. doi: 10.1088/1402-4896/ab95af.
[33] Kudryashov NA. One method for finding exact solutions of nonlinear differential equations. Commun Nonl Sci Numer Simulat. 2012;17(6):2248–53. doi: 10.1016/j.cnsns.2011.10.016.
[34] Pandir Y. A new approach to Kudryashovas method for solving some nonlinear physical models. Int J Phys Sci. 2012;7(21):2860. doi: 10.5897/ijps12.071.
[35] Brown PN, Hindmarsh A, Petzold LR. Using KryLov methods in the solution of large-scale differential-algebraic systems. SIAM J Sci Comput. 1994;15(6):1467–88. doi: 10.1137/0915088.
[36] Yao S, Akinyemi L, Mirzazadeh M, Inc M, Hosseini K, PPSSenol M. Dynamics of optical solitons in higher-order Sasa-Satsuma equation. Results Phys. 2021;30:104825. doi: 10.1016/j.rinp.2021.104825.
[37] Zayed EM, Amer YA, Shohib RM. The improved generalized Riccati equation mapping method and its application for solving a nonlinear partial differential equation (PDE) describing the dynamics of ionic currents along microtubules. Sci Res Essays. 2014;9(8):238–48. doi: 10.5897/sre2013.5772.
[38] Rani M, Ahmed N, Dragomir SS, Mohyud-Din ST, Khan I, Nisar KS. Some newly explored exact solitary wave solutions to nonlinear inhomogeneous Murnaghanas rod equation of fractional order. J Taibah Univ Sci. 2021;15(1):97–110. doi: 10.1080/16583655.2020.1841472.

[39] Alharbi A, Naire S. An adaptive moving mesh method for thin film flow equations with surface tension. J Comput Appl Math. 2017;319:365–84. doi: 10.1016/j.cam.2017.01.019.
[40] Alharbi A, Naire S. An adaptive moving mesh method for two-dimensional thin film flow equations with surface tension. J Comput Appl Math. 2019;356:219–30. doi: 10.1016/j.cam.2019.02.010.
[41] Alharbi A. Numerical solution of thin-film flow equations using adaptive moving mesh methods. Ph.D. Thesis. United Kingdom: Keele University. 2016. https://eprints.keele.ac.uk/id/eprint/2356.
[42] Cook S. Adaptive mesh methods for numerical weather prediction. Ph.D. Thesis. University of Bath; 2016. https://api.semanticscholar.org/CorpusID:125191178.
[43] Ismail, Mosally FM. A fourth order finite difference method for the good Boussinesq equation. Abstract Appl Anal. 2014;2014:1–10. doi: 10.1155/2014/323260.